

SHAPE SENSITIVITY AND RELIABILITY ANALYSES IN NONLINEAR FRACTURE MECHANICS

G. Chen and S. Rahman

Department of Mechanical Engineering, The University of Iowa,
Iowa City, IA 52242

ABSTRACT

This paper presents a new method for shape sensitivity analysis of a crack in a homogeneous, isotropic, and nonlinearly elastic body subject to mode-I loading conditions. The method involves the material derivative concept of continuum mechanics, domain integral representation of the J -integral, and direct differentiation. Unlike virtual crack extension techniques, no mesh perturbation is required in the proposed method. Based on the continuum sensitivities, the first-order reliability method was employed to perform probabilistic analysis. Numerical examples are presented to illustrate both the sensitivity and reliability analyses. The maximum difference between the sensitivity of stress-intensity factors calculated using the proposed method and the finite-difference method is less than four percent. Since all gradients are calculated analytically, the reliability analysis of cracks can be performed efficiently.

KEYWORDS

Shape sensitivity analysis, velocity field, J -integral, probabilistic fracture mechanics, reliability.

INTRODUCTION

In probabilistic fracture mechanics (PFM), the derivatives of the J -integral or stress-intensity factors (SIFs) are often required to predict the probability of fracture initiation and/or instability in cracked structures. The calculation of these derivatives with respect to load or material parameters, which constitutes size-sensitivity analysis, is not unduly difficult. However, the evaluation of derivatives with respect to crack size is a challenging task, since it requires shape sensitivity analysis. Using a brute-force type finite-difference method to calculate the shape sensitivities is often computationally expensive, because numerous deterministic finite element analyses may be required for a complete reliability analysis. Hence, some analytical methods have appeared to predict the sensitivities of SIFs under mode-I loading condition. For example, finite element methods (FEMs) based on virtual crack extension techniques have been developed to calculate the first- and second-order derivatives of SIFs [1]. However, these methods require mesh perturbation – a fundamental requirement of all virtual crack-extension techniques. For second-order derivatives, the number of elements affected by mesh perturbation surrounding the crack tip has a significant effect on solution accuracy [1]. Recently, alternative methods based on continuum sensitivity theory have emerged to obtain derivatives of SIFs for linear-elastic cracked structures [2,3]. No mesh perturbation is necessary in the latter formulation involving continuum shape sensitivity analysis.

However, these methods are valid only for linear-elastic structures. Hence, there is a need to develop similar sensitivity equations for nonlinear cracked structures.

This paper presents a new method for predicting the first-order sensitivity of the J -integral for a crack in a nonlinearly elastic structure under mode-I loading conditions. The method involves the material derivative concept of continuum mechanics, domain integral representation of the J -integral, and direct differentiation. Based on the proposed sensitivities, the first-order reliability method is employed for predicting stochastic response and reliability of cracked structures. Several numerical examples are presented for calculating both the sensitivity of the J -integral and reliability of cracked structures.

SHAPE SENSITIVITY ANALYSIS

The governing variational equation for a nonlinearly elastic structural component with the domain Ω can also be written as [4]

$$a_{\Omega}(\mathbf{z}, \bar{\mathbf{z}}) = \ell_{\Omega}(\bar{\mathbf{z}}), \quad \text{for all } \bar{\mathbf{z}} \in \mathbf{Z} \quad (1)$$

where \mathbf{z} and $\bar{\mathbf{z}}$ are the actual displacement and virtual displacement fields of the structure, respectively, \mathbf{Z} is the space of kinematically admissible virtual displacements, $a_{\Omega}(\mathbf{z}, \bar{\mathbf{z}})$ and $\ell_{\Omega}(\bar{\mathbf{z}})$ are energy and load linear forms, respectively. In Equations 1, $a_{\Omega}(\mathbf{z}, \bar{\mathbf{z}})$ is nonlinear and must be linearized by a_{Ω}^* (say) for iterative solution of \mathbf{z} . Taking the material derivative of the linearized form of Equation 1 yields,

$$a_{\Omega}^*(\mathbf{z}; \dot{\mathbf{z}}, \bar{\mathbf{z}}) = \ell'_{\mathbf{V}}(\bar{\mathbf{z}}) - a'_{\mathbf{V}}(\mathbf{z}, \bar{\mathbf{z}}), \quad \forall \bar{\mathbf{z}} \in \mathbf{Z}, \quad (2)$$

where the subscript \mathbf{V} is used to indicate the dependency of the terms on the velocity field [4], and

$$a_{\Omega}^*(\mathbf{z}; \dot{\mathbf{z}}, \bar{\mathbf{z}}) = \int_{\Omega} \frac{\partial \sigma_{ij}}{\partial \varepsilon_{kl}}(\dot{\mathbf{z}}) \varepsilon_{ij}(\bar{\mathbf{z}}) d\Omega \quad (3)$$

$$\ell'_{\mathbf{V}}(\bar{\mathbf{z}}) = \int_{\Gamma} \left\{ -T_i(z_{i,j} V_j) + [(T_i \bar{z}_i)_{,j} n_j + \kappa_{\Gamma}(T_i \bar{z}_i)] (V_i n_i) \right\} d\Gamma \quad (4)$$

$$a'_{\mathbf{V}}(\mathbf{z}, \bar{\mathbf{z}}) = - \int_{\Omega} \left[\frac{\partial \sigma_{ij}}{\partial \varepsilon_{kl}}(z_{k,m} V_{m,l}) \varepsilon_{ij}(\bar{\mathbf{z}}) + \sigma_{ij}(\mathbf{z})(\bar{z}_{i,m} V_{m,j}) - \sigma_{ij}(\mathbf{z}) \varepsilon_{ij}(\bar{\mathbf{z}}) \text{div} \mathbf{V} \right] d\Omega \quad (5)$$

where T_i is the i th component of the surface traction, V_i is the i th component of \mathbf{V} , n_i is the i th component of unit normal vector \mathbf{n} , and κ_{Γ} is the curvature of the boundary, and $z_{i,j} = \partial z_i / \partial x_j$, $\bar{z}_{i,j} = \partial \bar{z}_i / \partial x_j$, and $V_{i,j} = \partial V_i / \partial x_j$. For a performance measure ψ with a functional form

$$\psi = \int_{\Omega_{\tau}} g(\mathbf{z}_{\tau}, \nabla \mathbf{z}_{\tau}) d\Omega_{\tau}, \quad (6)$$

the material derivative of ψ at Ω is [4]

$$\dot{\psi} = \int_{\Omega} \left[g_{,z_i} \dot{z}_i - g_{,z_i}(z_{i,j} V_j) + g_{,z_{i,j}} \dot{z}_{i,j} - g_{,z_{i,j}}(z_{i,j} V_j)_{,j} + \text{div}(g \mathbf{V}) \right] d\Omega \quad (7)$$

where $z_{i,j} = \partial z_i / \partial x_j$, $\dot{z}_{i,j} = \partial \dot{z}_i / \partial x_j$, $g_{,z_i} = \partial g / \partial z_i$, $g_{,z_{i,j}} = \partial g / \partial z_{i,j}$ and V_j is the j th component of \mathbf{V} . To evaluate the sensitivity expression of Equation 7, a numerical method is needed to solve Equation 1. In this study, standard nonlinear FEM was used to solve Equation 1. However, the solution of $\dot{\mathbf{z}}$ can be obtained efficiently from Equation 2, since it is actually a linear system. Since the sensitivity equation is always linear even for nonlinear systems, the continuum shape sensitivity method is more efficient than the finite-difference method that requires solving at least two nonlinear systems of equations. In this study, the ABAQUS finite element code [5] was used for all numerical calculations.

THE J-INTEGRAL AND ITS SENSITIVITY

A widely used constitutive equation for J_2 -deformation theory of plasticity, usually under small-displacement conditions, is based on the well-known Ramberg-Osgood relation [6], given by

$$\varepsilon_{ij} = \frac{1+\nu}{E} s_{ij} + \frac{1-2\nu}{3E} \sigma_{kk} \delta_{ij} + \frac{3}{2} \alpha \varepsilon_0 \left(\frac{\sigma_e}{\sigma_0} \right)^{n-1} \frac{s_{ij}}{\sigma_0} \quad (8)$$

where σ_{ij} and ε_{ij} are stress and strain components, respectively, E is the Young's modulus, ν is Poisson's ratio, σ_0 is a reference stress, α is a dimensionless material constant, n is the strain hardening exponent, δ_{ij} is the Kronecker delta, $s_{ij} = \sigma_{ij} - \frac{1}{3} \sigma_{kk} \delta_{ij}$ is the deviatoric stress, and $\sigma_e = \sqrt{\frac{3}{2} s_{ij} s_{ij}}$ is the *von Mises* equivalent stress. The deformation theory assumes that the state of stress determines the state of strain uniquely as long as the plastic deformation continues. This is identical to the nonlinearly elastic stress-strain relation as long as unloading does not occur. This paper is concerned with the development of sensitivity equations for the J -integral using only the deformation theory of plasticity.

Under quasi-static condition, in the absence of body forces, thermal strains, and crack-face traction, the domain integration form of the J -integral for a two-dimensional problem is [6]

$$J = \int_A \left[\left(\sigma_{11} \frac{\partial z_1}{\partial x_1} + \sigma_{12} \frac{\partial z_2}{\partial x_1} \right) \frac{\partial q}{\partial x_1} + \left(\sigma_{21} \frac{\partial z_1}{\partial x_1} + \sigma_{22} \frac{\partial z_2}{\partial x_1} \right) \frac{\partial q}{\partial x_2} - W \frac{\partial q}{\partial x_1} \right] dA, \quad (9)$$

where W is the strain energy density, A is the area inside an arbitrary contour, q is a weight function which is unity at the outer boundary of A and zero at the crack tip. For a mode-I problem, the velocity field $\mathbf{V} = \{V_1, 0\}^T$. By applying the shape sensitivity concept described earlier, the sensitivity of J is

$$\dot{J} = \int_A (H_1 + H_2 + H_3 + H_4 - H_5) dA \quad (10)$$

where

$$H_1 = \frac{\partial z_1}{\partial x_1} \frac{\partial q}{\partial x_1} \left[\frac{\partial \sigma_{11}}{\partial \varepsilon_{11}} \left(\frac{\partial \dot{z}_1}{\partial x_1} - \frac{\partial z_1}{\partial x_1} \frac{\partial V_1}{\partial x_1} \right) + \frac{\partial \sigma_{11}}{\partial \varepsilon_{12}} \left(\frac{\partial \dot{z}_1}{\partial x_2} + \frac{\partial \dot{z}_2}{\partial x_1} - \frac{\partial z_1}{\partial x_1} \frac{\partial V_1}{\partial x_2} - \frac{\partial z_2}{\partial x_1} \frac{\partial V_1}{\partial x_1} \right) \right] \\ + \frac{\partial z_1}{\partial x_1} \frac{\partial q}{\partial x_1} \frac{\partial \sigma_{11}}{\partial \varepsilon_{22}} \left(\frac{\partial \dot{z}_2}{\partial x_2} - \frac{\partial z_2}{\partial x_1} \frac{\partial V_1}{\partial x_2} \right) + \sigma_{11} \frac{\partial q}{\partial x_1} \left(\frac{\partial \dot{z}_1}{\partial x_1} - \frac{\partial z_1}{\partial x_1} \frac{\partial V_1}{\partial x_1} \right) \quad (11)$$

$$H_2 = \frac{\partial z_2}{\partial x_1} \frac{\partial q}{\partial x_1} \left[\frac{\partial \sigma_{12}}{\partial \varepsilon_{11}} \left(\frac{\partial \dot{z}_1}{\partial x_1} - \frac{\partial z_1}{\partial x_1} \frac{\partial V_1}{\partial x_1} \right) + \frac{\partial \sigma_{12}}{\partial \varepsilon_{12}} \left(\frac{\partial \dot{z}_2}{\partial x_1} + \frac{\partial \dot{z}_1}{\partial x_2} - \frac{\partial z_2}{\partial x_1} \frac{\partial V_1}{\partial x_1} - \frac{\partial z_1}{\partial x_1} \frac{\partial V_1}{\partial x_2} \right) \right] \\ + \frac{\partial z_2}{\partial x_1} \frac{\partial q}{\partial x_1} \frac{\partial \sigma_{12}}{\partial \varepsilon_{22}} \left(\frac{\partial \dot{z}_2}{\partial x_2} - \frac{\partial z_2}{\partial x_1} \frac{\partial V_1}{\partial x_2} \right) + \sigma_{12} \frac{\partial q}{\partial x_1} \left(\frac{\partial \dot{z}_2}{\partial x_1} - \frac{\partial z_2}{\partial x_1} \frac{\partial V_1}{\partial x_1} \right) \quad (12)$$

$$H_3 = \frac{\partial z_1}{\partial x_1} \frac{\partial q}{\partial x_2} \left[\frac{\partial \sigma_{12}}{\partial \varepsilon_{11}} \left(\frac{\partial \dot{z}_1}{\partial x_1} - \frac{\partial z_1}{\partial x_1} \frac{\partial V_1}{\partial x_1} \right) + \frac{\partial \sigma_{12}}{\partial \varepsilon_{12}} \left(\frac{\partial \dot{z}_2}{\partial x_1} + \frac{\partial \dot{z}_1}{\partial x_2} - \frac{\partial z_2}{\partial x_1} \frac{\partial V_1}{\partial x_1} - \frac{\partial z_1}{\partial x_1} \frac{\partial V_1}{\partial x_2} \right) \right] \\ + \frac{\partial z_1}{\partial x_1} \frac{\partial q}{\partial x_2} \frac{\partial \sigma_{12}}{\partial \varepsilon_{22}} \left(\frac{\partial \dot{z}_2}{\partial x_2} - \frac{\partial z_2}{\partial x_1} \frac{\partial V_1}{\partial x_2} \right) + \sigma_{12} \frac{\partial q}{\partial x_2} \frac{\partial \dot{z}_1}{\partial x_1} - \sigma_{12} \frac{\partial q}{\partial x_1} \frac{\partial z_1}{\partial x_1} \frac{\partial V_1}{\partial x_2} \quad (13)$$

$$H_4 = \frac{\partial z_2}{\partial x_1} \frac{\partial q}{\partial x_2} \left[\frac{\partial \sigma_{22}}{\partial \varepsilon_{11}} \left(\frac{\partial \dot{z}_1}{\partial x_1} - \frac{\partial z_1}{\partial x_1} \frac{\partial V_1}{\partial x_1} \right) + \frac{\partial \sigma_{22}}{\partial \varepsilon_{12}} \left(\frac{\partial \dot{z}_2}{\partial x_1} + \frac{\partial \dot{z}_1}{\partial x_2} - \frac{\partial z_2}{\partial x_1} \frac{\partial V_1}{\partial x_1} - \frac{\partial z_1}{\partial x_1} \frac{\partial V_1}{\partial x_2} \right) \right] \\ + \frac{\partial z_2}{\partial x_1} \frac{\partial q}{\partial x_2} \frac{\partial \sigma_{22}}{\partial \varepsilon_{22}} \left(\frac{\partial \dot{z}_2}{\partial x_2} - \frac{\partial z_2}{\partial x_1} \frac{\partial V_1}{\partial x_2} \right) + \sigma_{22} \frac{\partial q}{\partial x_2} \frac{\partial \dot{z}_2}{\partial x_1} - \sigma_{22} \frac{\partial q}{\partial x_1} \frac{\partial z_2}{\partial x_1} \frac{\partial V_1}{\partial x_2} \quad (14)$$

$$H_5 = \frac{\partial q}{\partial x_1} \frac{\partial W}{\partial \sigma_{ij}} \left[\frac{\partial \sigma_{ij}}{\partial \epsilon_{11}} \left(\frac{\partial z_1}{\partial x_1} - \frac{\partial z_1}{\partial x_1} \frac{\partial V_1}{\partial x_1} \right) + \frac{\partial \sigma_{ij}}{\partial \epsilon_{22}} \left(\frac{\partial z_2}{\partial x_2} - \frac{\partial z_2}{\partial x_1} \frac{\partial V_1}{\partial x_2} \right) \right] + \frac{\partial q}{\partial x_1} \frac{\partial W}{\partial \sigma_{ij}} \frac{\partial \sigma_{ij}}{\partial \epsilon_{12}} \left(\frac{\partial z_2}{\partial x_1} + \frac{\partial z_1}{\partial x_2} - \frac{\partial z_1}{\partial x_1} \frac{\partial V_1}{\partial x_2} - \frac{\partial z_2}{\partial x_1} \frac{\partial V_1}{\partial x_1} \right) \quad (15)$$

Equations 11-15 are valid for both plane stress and plane strain conditions and can be inserted in Equation 10 to yield the first-order sensitivity of J with respect to crack size. The integral in Equation 10 is independent of the domain size and can be calculated numerically using the standard Gaussian quadrature. A 2×2 or higher integration rule is recommended for calculating \dot{J} .

FRACTURE RELIABILITY ANALYSIS

Consider a cracked structure with uncertain mechanical and geometric characteristics that is subject to random loads. Denote by \mathbf{X} an N -dimensional random vector with components X_1, X_2, \dots, X_N characterizing all uncertainty in load, geometry, and material parameters. Let J be a relevant crack-driving force that can be calculated from FEM. Suppose, the structure fails when $J > J_{Ic}$, where J_{Ic} is the mode-I plane strain fracture toughness of the material. This requirement cannot be satisfied with certainty, because J depends on input \mathbf{X} which is random and J_{Ic} itself is a random variable. Hence, the performance of the cracked structure should be evaluated by the probability of failure P_F , defined as

$$P_F \stackrel{\text{def}}{=} \Pr[g(\mathbf{X}) < 0] \stackrel{\text{def}}{=} \int_{g(\mathbf{x}) < 0} f_{\mathbf{X}}(\mathbf{x}) d\mathbf{x} \quad (16)$$

where $f_{\mathbf{X}}(\mathbf{x})$ is the joint probability density function of \mathbf{X} , and $g(\mathbf{X}) = J_{Ic}(\mathbf{X}) - J(\mathbf{X})$ is the performance function. The failure probability in Equation 16 involves multi-fold probability integration for its evaluation. In this study, the first-order reliability method (FORM) [7] was used to compute this probability. The calculation of failure probability in the context of FORM can be viewed as a constrained nonlinear optimization problem, which in turn requires first-order sensitivities of J with respect to all random parameters. The proposed shape sensitivity method can be effectively applied to FORM when the crack size is modeled as a random parameter.

NUMERICAL EXAMPLES

Example 1: Sensitivity Analysis of M(T) and SE(T) Specimens

Consider a middle-tension [M(T)] and a single-edged-tension [SE(T)] specimens with width, $2W = 1.016$ m, length, $2L = 5.08$ m and a crack length, $2a$, that are subjected to far-field remote tensile stress, $\sigma^\infty = 172.4$ MPa. Two distinct crack sizes with normalized crack lengths, $a/W = 0.25$ and 0.5 were considered for both specimens. For material properties: reference stress, $\sigma_0 = 154.8$ MPa; elastic modulus, $E = 207$ GPa; Poisson's ration, $\nu = 0.3$; and Ramberg-Osgood parameters, $\alpha = 8.073$ and $n = 3.8$. Figures 1 and 2 show the geometry and loads of the M(T) and SE(T) specimens, respectively. A finite element mesh for 1/2 model of the SE(T) specimen and 1/4 model of the M(T) specimen is shown in Figure 3. A plane stress condition was assumed. Second-order, eight-noded quadrilateral elements from ABAQUS [5] library were used. The number of elements and nodes were 208 and 691, respectively. Focused elements with collapsed nodes were employed in the vicinity of crack tip. A 2×2 Gaussian integration was used.

Tables 1 and 2 show the results of J and $\partial J / \partial a$ for M(T) and SE(T) problems, respectively. For $\partial J / \partial a$, two sets of results are shown. One is based on the proposed sensitivity method described in this thesis. The other is based on the finite-difference method using a one-percent perturbation of crack length. The results of Tables 1 and 2 show that the continuum sensitivity method provides very accurate results of

$\partial J/\partial a$ when compared with the corresponding results of the finite-difference method. Unlike the virtual crack extension techniques, no mesh perturbation is needed in the proposed method. The difference between the results of the proposed method and the finite-difference method is less than four percent.

Example 2: Reliability Analysis of DE(T) Specimen

Consider a double-edged-tension [DE(T)] specimen with width, $2W = 1.016$ m, length, $2L = 5.08$ m, and random crack length, a . It is subject to a far-field tensile stress, σ^∞ , as shown in Figure 4. The load (σ^∞), crack size (a/W), and material properties (E , α , and J_{Ic}) were treated as statistically independent random variables with their properties listed in Table 3. The Poisson’s ratio, $\nu = 0.3$ and the Ramberg-Osgood exponent, $n = 3.8$ were assumed to be deterministic. The same finite element mesh of Figure 3 was used for this DE(T) specimen (at mean crack length) for 1/4 model. A plane stress condition was assumed.

Using continuum sensitivity of J and FORM, reliability analyses were conducted to calculate the probability of failure P_F , as a function of mean far-field tensile stress $E[\sigma^\infty]$. Figure 5 shows the plots of P_F vs. $E[\sigma^\infty]$ for both deterministic ($v_{a/W} = 0$) and random ($v_{a/W} = 10, 20$ percent) crack sizes, where $v_{a/W}$ denotes the coefficient of variation (COV) of a/W . The results indicate that the failure probability increases with the COV (uncertainty) of a/W as expected and can be much larger than the probabilities calculated for a deterministic crack size, particularly when the uncertainty of a/W is large. For $v_{a/W} = 10$ percent, failure probability was also calculated by Monte Carlo simulation with the sample size at least 10 times the inverse of failure probability being estimated. According to Figure 5, the probability of failure by FORM is in good agreement with the simulation results.

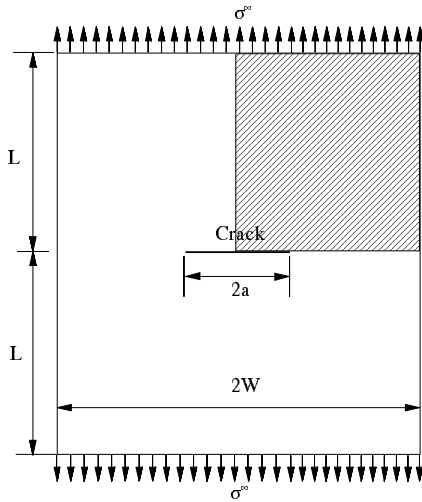


Figure 1: M(T) specimen

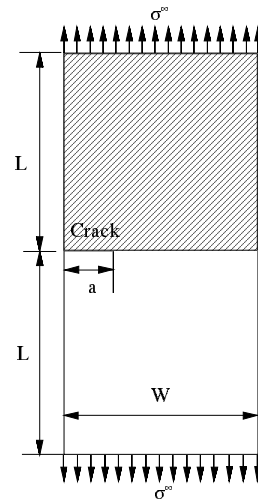


Figure 2: SE(T) specimen

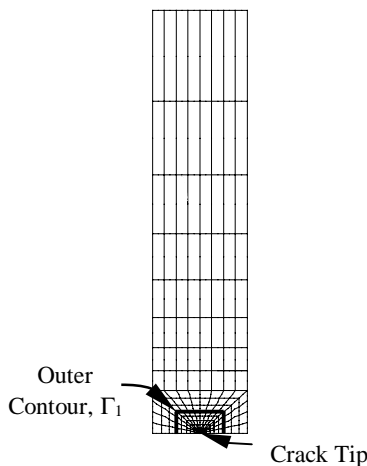


Figure 3: Finite element mesh

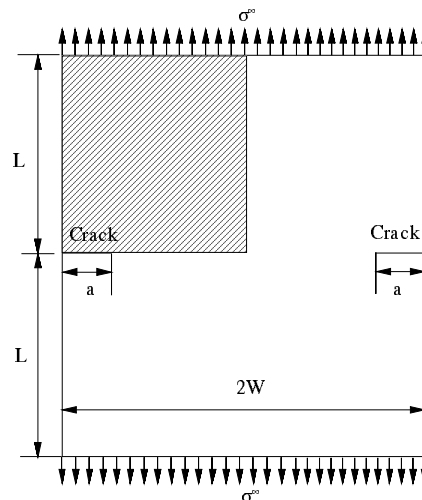


Figure 4: DE(T) specimen

TABLE 1
SENSITIVITY OF J FOR M(T) SPECIMEN

a/W	J kJ/m ²	Sensitivity of J ($\partial J/\partial a$) kJ/m ³		
		Prop. Method	Finite Diff.	Diff. %
0.25	2.00×10^3	27.6×10^3	26.8×10^3	2.87
0.5	11.2×10^3	17.2×10^4	17.6×10^4	-2.73

TABLE 2
SENSITIVITY OF J FOR SE(T) SPECIMEN

a/W	J kJ/m ²	Sensitivity of J ($\partial J/\partial a$) kJ/m ³		
		Prop. Method	Finite Diff.	Diff. %
0.25	6.20×10^3	14.7×10^4	14.4×10^4	1.82
0.5	3.70×10^5	17.1×10^6	16.6×10^6	3.29

TABLE 3
STATISTICAL PROPERTIES OF INPUT

Random Variable	Mean	COV	Probability Distribution
a/W	0.5	0-0.2	Uniform
E	207 GPa	0.05	Gaussian
α	8.073	0.1439	Lognormal
σ^∞	40-110 MPa	0.1	Gaussian
J_{Ic}	1243 kJ/m ²	0.47	Lognormal

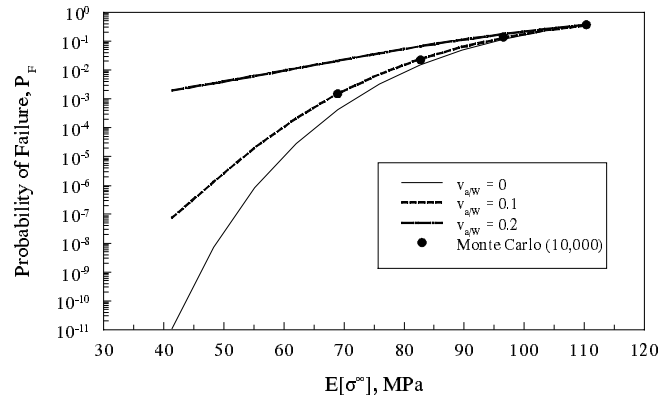


Figure 5: Failure probability of DE(T)

CONCLUSIONS

A new method was developed for continuum shape sensitivity analysis of a crack in a homogeneous, isotropic, nonlinearly elastic body subject to mode-I loading conditions. The method involves the material derivative concept of continuum mechanics, domain integral representation of the J -integral, and direct differentiation. Unlike virtual crack extension techniques, no mesh perturbation is required in the proposed method. Numerical examples have been presented to illustrate the proposed method. The results show that the maximum difference between the sensitivity of stress-intensity factors calculated using the proposed method and reference solutions obtained by the finite-difference method is less than four percent. Based on the continuum sensitivities, the first-order reliability method was formulated to perform probabilistic fracture-mechanics analysis. A numerical example is presented to illustrate the usefulness of the proposed sensitivity equations for probabilistic analysis. Since all gradients are calculated analytically, the reliability analysis of cracks can be performed efficiently.

REFERENCES

1. Hwang, C., Wawrzynek, P., Tayebi, A., and Ingraffea, A. (1998), *Engng. Frac. Mech.*, 59, 521.
2. Chen, G., Rahman, S., and Park, Y. H. (2001), accepted in *Comp. Mech.*
3. Taroco, E. (2000), *Comp. Meth. Appl. Mech. Engng.*, 188 (4), 697.
4. Haug, E., Choi, K., and Komkov, V. (1986), *Design Sensitivity Analysis of Structural Systems*, Academic Press, New York.
5. ABAQUS (2000), *User's Guide and Theoretical Manual*, Version 5.8, Hibbit, Karlsson, and Sorenson, Inc., Pawtucket, Rhode Island.
6. Anderson, T. L. (1995), *Fracture Mechanics - Fundamentals and Applications*, CRC Press.
7. Madsen, H., Krenk, S., and Lind, N. (1986), *Methods of Structural Safety*, Prentice-Hall, Inc., Englewood Cliffs, New Jersey.